Characteristic Impedances of Multiconductor Strip Transmission Lines

J. W. DUNCAN, SENIOR MEMBER, IEEE

Abstract—The design of certain log-periodic microwave circuit elements requires a knowledge of the characteristic impedances of a system of four-coupled strip transmission lines.[1] The system of four strip conductors between parallel ground planes is capable of supporting four different TEM modes which have different characteristic impedances. In this paper, the characteristic impedances of the four modes are determined by a variational method. The variational solution is an upper bound to the exact characteristic impedance of the line.

In general, the coplanar strip conductors are located at an arbitrary (but identical) displacement from the parallel ground planes. When the separation between the broadside-coupled strips is precisely one-half the spacing between the parallel ground planes, two of the mode impedances may be determined exactly by means of conformal mapping. The variational solutions are compared to the exact solutions for this special case. Because of the "cell image" principle which holds for the problem, the mode solutions presented here also apply to various single- and two-conductor strip transmission lines with arbitrary displacements. As a result, solutions for the following strip line configurations are available from the analysis: a single strip conductor in a trough, or between parallel ground planes; two coplanar strips between ground planes; two broadside-coupled strips in a trough, or between parallel ground planes. An extensive set of curves are presented which show the characteristic impedances of the four modes as a function of the relative dimensions of the strip transmission line.

Introduction

We ASSUME a lossless transmission line of uniform cross section so that the electromagnetic problem reduces to solving Laplace's equation in the transverse plane. A cross-sectional view of the four conductor strip line is shown in Fig. 1. The medium between the plates is considered homogeneous and isotropic with inductive capacities $\mu=\mu_0$ and $\epsilon=\epsilon_r\epsilon_0$, where $\mu_0=4\pi\times10^{-7}$ henry/meter and $\epsilon_0=1/36\pi\times10^{-9}$ farad/meter are free space capacities, and ϵ_r is the relative dielectric constant. Under these conditions, all mode solutions are TEM fields which propagate with the velocity $v=(\mu\epsilon)^{-1/2}$ characteristic of the medium. The characteristic impedance of the transmission line for a particular mode is given by $(vC)^{-1}$, where C is the electrostatic capacitance per unit length between the conductors. The capacitance and, therefore, the characteristic impedance, will depend upon how potential is applied to the system of conductors. In Fig. 2, we use polarity signs to show the four ways in which the potential ϕ_0 (volts) is applied to the strip conductors. The parallel ground planes are of infinite extent and are at zero potential relative to the strip conductors. The "cell" characteristic impedances for the four modes of excitation are denoted Z_{01}, Z_{02}, Z_{03}, and Z_{04}. For a particular mode, the characteristic impedance is determined uniquely by the intrinsic impedance of the medium $(\mu/\epsilon)^{1/2}$, and the relative line dimensions τ/b, w/b, and η/b, which are the line dimensions shown in Fig. 1 normalized with respect to $2b$, the separation of the parallel ground planes.

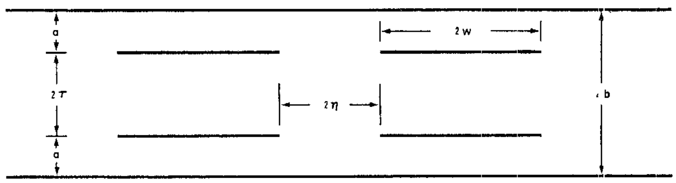

Fig. 1. Four-conductor strip transmission line.

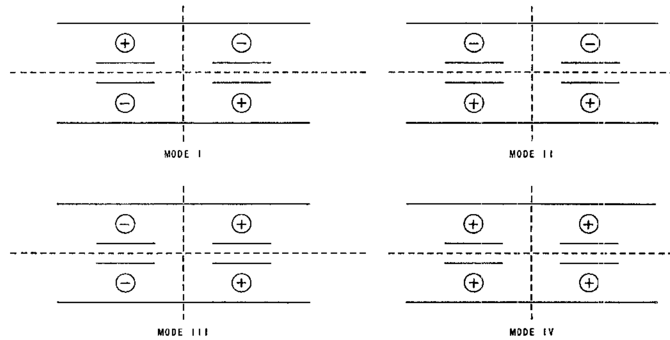

Fig. 2. Fundamental modes for four-conductor strip line.

As a consequence of the strip line geometry and the symmetry of applied potentials, the dashed lines bisecting the cross sections in Fig. 2 are the positions of electric or magnetic walls, depending upon the relative excitation between conductors. At an electric wall, the electric field is entirely normal ($\bar{E}\times\bar{n}=0$), while at a magnetic wall, the electric field is entirely tangential ($\bar{E}\cdot\bar{n}=0$). The dashed line is an electric wall or a magnetic wall as it bisects potentials of the opposite or same sign, respectively. In terms of the potential function $\phi(x, y)$, $\phi=0$ at an electric boundary and $\partial\phi/\partial n=0$ at a magnetic boundary. For any mode, the dashed lines divide the cross section into four "cells" which are, in effect, images of each other. In order to determine the characteristic impedance of the four conductor system, it is sufficient, therefore, to solve the static field problem for a single cell. The impedance obtained for the single cell is identical to the impedance of the

Manuscript received July 27, 1964; revised October 2, 1964. The work described in this paper was partially supported by the U. S. Naval Ordnance Laboratory, Corona, Calif. under Contract N123-(62738)50145A.

The author is with the Electromagnetics Staff, Radar Div., Ground Systems Group, Hughes Aircraft Co., Fullerton, Calif.

[1] DuHamel, R. H., Symmetry analysis of waveguide junctions: Application to log-periodic circuits, ID 63-14-108, Ground Systems Group, Hughes Aircraft Co., Fullerton, Calif., Jul 11, 1963.

four conductor system in the case of Modes I, II, and III. In the case of Mode IV, the four conductor impedance is one-quarter the cell impedance.

Mode I

In Fig. 3, we show a cell of the line cross section with boundary conditions appropriate for Mode I. The dimensions are consistent with those defined in Fig. 1. The semi-infinite parallel plates at $y=0$ and $y=b$, in conjunction with the electric wall at $x=0$, $0 \leq y \leq b$ defines a semi-infinite trough transmission line. The zero-thickness strip conductor of width $2w$ extends from $x=\eta$ to $x=\xi$ at a position $y=a$, where $0<a<b$. The midpoint of the strip is $x=h$, so that $\xi=h+w$ and $\eta=h-w$. Referring to Fig. 1, the normalized dimension $\eta/b=h/b-w/b$, and the dimension $\tau/b=(2b-2a)/2b=1-a/b$.

A potential ϕ_0 is applied to the strip and the potential is zero on the walls of the trough. A variational expression for the characteristic impedance of the strip line may be written in terms of the unknown charge distribution of the strip conductor.[2] First, we require the potential (Green's function) resulting from a unit line charge located at a point x', y' in the trough region of Fig. 3. The Green's function is defined by the inhomogeneous equation

$$\frac{\partial^2 G}{\partial x^2}+\frac{\partial^2 G}{\partial y^2}=-\frac{1}{\epsilon}\delta(x-x')\delta(y-y') \tag{1}$$

where the two-dimensional delta function $\delta(x-x')\delta(y-y')$ represents the unit source at x', y'. The boundary conditions on G are

$$\begin{array}{llll} G=0 & \text{for} & x=0, & 0\leq y\leq b \\ G\rightarrow 0 & \text{as} & x\rightarrow\infty, & 0<y<b \\ G=0 & \text{for} & x\geq 0, & y=0 \\ & & & y=b \end{array} \tag{2}$$

The function $G(x, y|x', y')$ which satisfies (1) and (2) is

$$G_1(x, y \mid x', y') = \frac{2}{\epsilon\pi}\sum_{n=1}^{\infty}\frac{1}{n}\sin\left(\frac{n\pi y}{b}\right)\sin\left(\frac{n\pi y'}{b}\right) \cdot \begin{cases} e^{-n\pi x'/b}\sinh\left(\frac{n\pi x}{b}\right), & x\leq x' \\ e^{-n\pi x/b}\sinh\left(\frac{n\pi x'}{b}\right), & x\geq x' \end{cases} \tag{3}$$

where the notation G_1 signifies that the Green's function derives from the boundary conditions for Mode I.

The charge per unit area $\sigma(x')$ on the surface of the strip conductor is a one-dimensional charge distribution (per unit length) over $y'=a$, $\eta\leq x'\leq\xi$. The potential at a point x, y resulting from the charge on the strip conductor is given by the integral

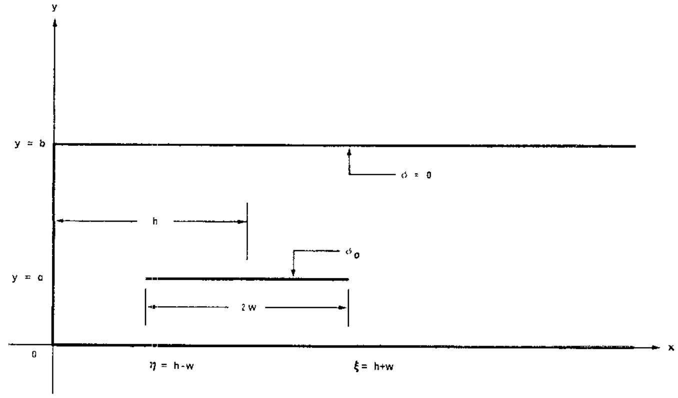

Fig. 3. Strip-line cell with Mode I boundary conditions.

$$\phi(x, y) = \int_\eta^\xi G_1(x, y \mid x', a)\sigma(x')dx' \tag{4}$$

When the point x, y is restricted to the position of the strip conductor, $\phi(x, y)$ must reduce to ϕ_0 the potential on the strip, hence

$$\phi_0 = \int_\eta^\xi G_1(x, a \mid x', a)\sigma(x')dx',$$

where

$$\eta \leq x \leq \xi \tag{5}$$

$G_1(x, a|x', a)$ which appears in (5) is obtained by setting $y=y'=a$ in (3), thus

$$G_1(x, a \mid x', a) = \frac{2}{\epsilon b}\sum_{n=1}^{\infty}\frac{\sin^2(ka)}{k}\begin{cases} e^{-kx'}\sinh(kx), & x\leq x' \\ e^{-kx}\sinh(kx'), & x\geq x' \end{cases} \tag{6}$$

where $k=n\pi/b$. Multiplying (5) by $\sigma(x)$ and integrating over the strip conductor yields

$$\phi_0 Q = \int_\eta^\xi\int_\eta^\xi G_1(x, a \mid x', a)\sigma(x)\sigma(x')dx'dx \tag{7}$$

where

$$Q = \int_\eta^\xi \sigma(x)dx$$

is the charge per unit length on the strip conductor. In MKS units, $\phi_0 Q$ has the dimensions volt-coulomb/meter.

The variational formula for impedance is obtained from the relation

$$Z_0 = (vC)^{-1} = (\mu\epsilon)^{1/2}\frac{\phi_0 Q}{Q^2} \tag{8}$$

Substituting (7) into (8) yields

[2] Collin, R. E., *Field Theory of Guided Waves*. New York: McGraw-Hill, 1960, pp 148–165.

$$Z_{01} = (\mu\epsilon)^{1/2} \frac{\int_\eta^\xi \int_\eta^\xi G_1(x, a \mid x', a)\sigma(x)\sigma(x')dx'dx}{\left[\int_\eta^\xi \sigma(x)dx\right]^2} \tag{9a}$$

$$= (\mu\epsilon)^{1/2} \frac{N}{Q_2} \tag{9b}$$

Where $N=\phi_0 Q$ represents the double integral in the numerator of (9a) that is, (7).

The stationary value of (9) is an absolute minimum, so that (9) provides an "upper bound" to the exact characteristic impedance of the line. The characteristic impedance is evaluated by substituting an approximate representation for $\sigma(x)$ in (9), and then minimizing Z_{01} with respect to the variational parameters a_i. This is accomplished by setting $\partial Z_{01}/\partial a_i = 0$, solving for the parameters a_i, and then substituting the a_i back into (9) to determine Z_{01}. We represent $\sigma(x')$ by the three-term series.

$$\sigma(x') = a_0 + a_1 x' + a_2 x'^2 \tag{10}$$

The general functional form of $\sigma(x')$ is an asymmetric parabolic distribution. From (10), the product $\sigma(x) \cdot \sigma(x')$ which appears in N is

$$\sigma(x)\sigma(x') = a_0^2 + a_0 a_1(x + x') + a_0 a_2(x^2 + x'^2) + a_1^2 xx' + a_1 a_2(x'x^2 + xx'^2) + a_2^2(x^2 x'^2) \tag{11}$$

At this point, it is convenient to introduce the functions Σ_i. Let the six functions Σ_i $(i=0, 1, 2, \cdots, 5)$ represent the following integrals

$$\left.\begin{aligned} \Sigma_0 &= \int_\eta^\xi \int_\eta^\xi G_1 dx'dx \\ \Sigma_1 &= \int_\eta^\xi \int_\eta^\xi x' G_1 dx'dx \\ \Sigma_2 &= \int_\eta^\xi \int_\eta^\xi x'^2 G_1 dx'dx \\ \Sigma_3 &= \int_\eta^\xi \int_\eta^\xi xx' G_1 dx'dx \\ \Sigma_4 &= \int_\eta^\xi \int_\eta^\xi xx'^2 G_1 dx'dx \\ \Sigma_5 &= \int_\eta^\xi \int_\eta^\xi x^2 x'^2 G_1 dx'dx \end{aligned}\right\} \tag{12}$$

where $G_1(x, a \mid x', a)$ is defined in (6). Because of the symmetry of the Green's function, x' and x may be interchanged in any of the integrals (12) without altering the value of the integral. From (9), we have

$$N = \int_\eta^\xi \int_\eta^\xi G_1(x, a \mid x', a)\sigma(x)\sigma(x')dx'dx \tag{13}$$

Substituting (11) into (13), we determine by virtue of of the definitions (12) and the Green's function symmetry that N is equal to

$$N = a_0^2\Sigma_0 + 2a_0 a_1 \Sigma_1 + 2a_0 a_2 \Sigma_2 + a_1^2 \Sigma_3 + 2a_1 a_2 \Sigma_4 + a_2^2 \Sigma_5 \tag{14}$$

The evaluation of the Σ_i integrals is straightforward and will not be presented here.[3] It results that the Σ_i functions are comprised of twenty-five fundamental infinite series which are denoted $S_{i\nu}$.[4] These series arise because of the series form of the Green's function. The simplest integral is Σ_0. In terms of the series $S_{i\nu}$, Σ_0 is given by

$$\Sigma_0 = \frac{2}{\epsilon b}\left[(\xi - \eta)S_{02} - S_{03} + S_{13} + S_{23} - \tfrac{1}{2}(S_{33} + S_{43})\right] \tag{15}$$

where, for example,

$$S_{13} = \sum_{n=1}^{\infty} \frac{\sin^2 (ka) e^{-k(\xi-\eta)}}{k^3} \tag{16}$$

Substituting (10) into the integral for Q yields

$$Q = \int_\eta^\xi \sigma(x)dx = 2w(a_0 + a_1 h + a_2 \gamma), \quad \text{coulomb/meter} \tag{17}$$

where $h=(\xi+\eta)/2$ is the midpoint of the strip, and $\gamma = h^2 + (w^2/3)$. When (14) and (17) are substituted into (9b), and Z_{01} is minimized with respect to the parameters a_i, a solution of the equations is

$$\left.\begin{aligned} a_0 &= 1 \\ a_1 &= \frac{K_{22}C_1 - K_{12}C_2}{K_{11}K_{22} - K_{21}K_{12}} \\ a_2 &= \frac{K_{11}C_2 - K_{21}C_1}{K_{11}K_{22} - K_{21}K_{12}} \end{aligned}\right\} \tag{18}$$

where

$$\begin{aligned} K_{11} &= \Sigma_3 - h\Sigma_1 & C_1 &= h\Sigma_0 - \Sigma_1 \\ K_{12} &= \Sigma_4 - h\Sigma_2 & C_2 &= \gamma\Sigma_0 - \Sigma_2 \\ K_{21} &= \Sigma_4 - \gamma\Sigma_1 & & \\ K_{22} &= \Sigma_5 - \gamma\Sigma_2 & & \end{aligned} \tag{19}$$

[3] For details see Duncan, J. W., Characteristic impedances of multiconductor strip transmission lines, FR 64-14-153, Hughes Aircraft Co., Ground Systems Group, Fullerton, Calif., Aug 7, 1964.

[4] The functions Σ_i and the series $S_{i\nu}$ are defined in the Appendix.

Substituting (14) and (17) into (9b) along with $a_0=1$, $\mu=\mu_0$, and $\epsilon=\epsilon_r\epsilon_0$, we obtain the result

$$\sqrt{\epsilon_r}\, Z_{01} = 120\pi \frac{\epsilon N}{Q^2} = 120\pi\epsilon \left\{ \frac{\Sigma_0 + 2a_1\Sigma_1 + 2a_2\Sigma_2 + a_1^2\Sigma_3 + 2a_1a_2\Sigma_4 + a_2^2\Sigma_5}{4w^2\left[1 + a_1 h + a_2\left(h^2 + \frac{w^2}{3}\right)\right]^2} \right\} \text{ohms} \tag{20}$$

where ϵ_r is the relative dielectric constant and $\sqrt{\mu_0/\epsilon_0} = 120\pi$ ohms. In (20), $\epsilon N = \epsilon\phi_0 Q$ has the dimensions (coulomb/meter)^2 and, therefore, $\epsilon N/Q^2$ is dimensionless.

Equation (20) is the variational solution for the characteristic impedance of the strip line cell which is depicted in Fig. 3. In order to evaluate (20), one must specify the dimensions a, b, h, and w. The twenty-five infinite series $S_{i\nu}$ must be evaluated, and then be used to form the six functions Σ_1. After the Σ_i functions have been determined, the variational parameters a_1 and a_2 may be calculated using (18) and (19). The variables are then substituted into (20) to obtain the characteristic impedance.

We wish to emphasize that the impedance is uniquely determined by the *relative* dimensions a/b, h/b, and w/b. Unfortunately, it is not evident that this condition exists when one views (20). The dependence of (20) upon relative dimensions is obscured because of the the manner in which $\sigma(x)$ was defined. It may be seen from (10) and (17) that the coefficients a_0, a_1, and a_2 have different dimensions. The definition (10) leads to the recondite form of (20). If we had chosen to define $\sigma(x)$ in the normalized form $\sigma(x)=a_0+a_1(x/b)+a_2(x/b)^2$, the dimensions of the coefficients a_i would be identical and the denominator of (20) would take on the new form $Q^2=4w^2\{a_0+a_1(h/b)+a_2[(h/b)^2+\frac{1}{3}(w/b)^2]\}^2$. The dependence of Z_{01} upon relative dimensions would then be more evident although the complicated nature of the Σ_i functions still makes this identification a difficult task. In any event, the choice in defining $\sigma(x)$ is completely arbitrary.

Mode II

The analysis of Mode II holds for the same cell geometry as Mode I (Fig. 3). The Green's function is still defined by (1), but the boundary conditions on the cell are the following:

$$\left.\begin{array}{llll} \dfrac{\partial G}{\partial x} = 0 & \text{for} & x = 0 & 0 \le y \le b \\ G \to 0 & \text{as} & x \to \infty & 0 < y < b \\ G = 0 & \text{for} & x \ge 0 & y = 0 \\ & & & y = b \end{array}\right\} \tag{21}$$

The function $G_2(x, y|x', y')$ which satisfies (1) and (21) is

$$G_2(x, y \mid x', y') = \frac{2}{\epsilon\pi}\sum_{n=1}^{\infty}\frac{1}{n}\sin\left(\frac{n\pi y}{b}\right)\sin\left(\frac{n\pi y'}{b}\right) \begin{cases} e^{-n\pi x'/b}\cosh\left(\dfrac{n\pi x}{b}\right) & x \le x' \\ e^{-n\pi x/b}\cosh\left(\dfrac{n\pi x'}{b}\right) & x \ge x' \end{cases} \tag{22}$$

It is convenient to define six functions Ξ_i which are integrals of $G_2(x, a|x', a)$ identical to the integrals of $G_1(x, a|x', a)$ defined in (12), that is let

$$\left.\begin{array}{l} \Xi_0 = \displaystyle\int_\eta^\xi\int_\eta^\xi G_2 dx' dx \\ \Xi_1 = \displaystyle\int_\eta^\xi\int_\eta^\xi x' G_2 dx' dx \\ \quad\vdots \\ \Xi_5 = \displaystyle\int_\eta^\xi\int_\eta^\xi x^2 x'^2 G_2 dx' dx \end{array}\right\} \tag{23}$$

Now it results that the functions Ξ_i are comprised of the same twenty-five infinite series $S_{i\nu}$ that form the functions Σ_i, the only difference being changes in sign of certain of the $S_{i\nu}$ terms. Consequently, it is convenient to define the functions Σ_i and Ξ_i simultaneously by means of the dual sign notation $(\pm)$.[5] The expression for Ξ_0 is

$$\Xi_0 = \frac{2}{\epsilon b}\left[(\xi - \eta)S_{02} - S_{03} + S_{13} - S_{23} + \tfrac{1}{2}(S_{33} + S_{43})\right] \tag{24}$$

which may be compared to (15), the expression for Σ_0. Now it should be evident that the analysis carried out for Mode I also applies to Mode II. The variational solution for Z_{02} may be written from (20) simply by replacing Σ_i by Ξ_i; hence,

[5] See the Appendix.

$$\sqrt{\epsilon_r}\, Z_{02} = 120\pi\epsilon\left\{\frac{\Xi_0 + 2a_1\Xi_1 + 2a_2\Xi_2 + a_1^2\Xi_3 + 2a_1a_2\Xi_4 + a_2^2\Xi_5}{4w^2\left[1 + a_1h + a_2\left(h^2 + \frac{w^2}{3}\right)\right]^2}\right\} \text{ohms} \tag{25}$$

where a_1 and a_2 are given by (18), but *the coefficients* K_{ij} *and* C_i *defined in (19) now must be constructed using* Ξ_i. For example, $K_{11}=\Xi_3-h\Xi_1$, and $C_2=\gamma\Xi_0-\Xi_2$.

Mode III

The cell geometry of Fig. 3 still applies, but the cell boundary conditions for Mode III are

$$\left.\begin{array}{llll} G = 0 & \text{for} & x = 0 & 0 \le y \le b \\ G = 0 & \text{for} & x \ge 0 & y = 0 \\ G \to 0 & \text{as} & x \to \infty & 0 < y < b \\ \dfrac{\partial G}{\partial y} = 0 & \text{for} & x \ge 0 & y = b \end{array}\right\} \tag{26}$$

From (1) and (26), the Green's function for Mode III is

$$G_3(x, y \mid x', y') = \frac{2}{\epsilon\pi}\sum_{n=1,3,5,\cdots}^{\infty}\frac{2}{n}\sin\left(\frac{n\pi y}{2b}\right)\sin\left(\frac{n\pi y'}{2b}\right)\cdot\begin{cases} e^{-n\pi x'/2b}\sinh\left(\dfrac{n\pi x}{2b}\right) & x \le x' \\ e^{-n\pi x/2b}\sinh\left(\dfrac{n\pi x'}{2b}\right) & x \ge x' \end{cases} \tag{27}$$

We may define integrals of $G_3(x, a \mid x', a)$ identical to the integrals of $G_1(x, a \mid x', a)$ defined in (12). When the integrals are evaluated, we find that the expressions are exactly the same as the functions Σ_i with the following change: the twenty-five infinite series in the expressions are similar to the series $S_{i\nu}$, except that the eigenvalue $k=n\pi/b$ is replaced by $k/2$ everywhere and the summation is restricted to the odd integers. These companion series to the $S_{i\nu}$ are denoted $\chi_{i\nu}$.[6] To illustrate, the function Σ_0 for Mode III is defined

$$\Sigma_0 = \int_\eta^\xi\int_\eta^\xi G_3(x, a \mid x', a)dx'dx$$
$$= \frac{2}{\epsilon b}\left[(\xi-\eta)\chi_{02} - \chi_{03} + \chi_{13} + \chi_{23} - \tfrac{1}{2}(\chi_{33} + \chi_{43})\right] \tag{28}$$

where, for example,

$$\chi_{13} = \sum_{n=1,3,5,\cdots}^{\infty}\frac{\sin^2\left(\dfrac{ka}{2}\right)e^{-k(\xi-\eta)/2}}{\left(\dfrac{k}{2}\right)^3} \tag{29}$$

[6] The series $\chi_{i\nu}$ are defined in the Appendix.

Expressions (28) and (29) may be compared to (15) and (16) which apply to Mode I.

The solution for Mode III follows directly from the analysis for Mode I. Z_{03} *is given by (20) when the functions* Σ_i, *and the parameters* a_1 *and* a_2 *are derived from the series* $\chi_{i\nu}$.

Mode IV

The boundary conditions for Mode IV on the cell geometry of Fig. 3 are

$$\left.\begin{array}{llll} G = 0 & \text{for} & x \ge 0 & y = 0 \\ G \to 0 & \text{as} & x \to \infty & 0 < y < b \\ \dfrac{\partial G}{\partial x} = 0 & \text{for} & x = 0 & 0 \le y \le b \\ \dfrac{\partial G}{\partial y} = 0 & \text{for} & x > 0 & y = b \end{array}\right\} \tag{30}$$

From (1) and (30), the Green's function for Mode IV is

$$G_4(x, y \mid x', y') = \frac{2}{\epsilon\pi}\sum_{n=1,3,5,\cdots}^{\infty}\frac{2}{n}\sin\left(\frac{n\pi y}{2b}\right)\sin\left(\frac{n\pi y'}{2b}\right)\cdot\begin{cases} e^{-n\pi x'/2b}\cosh\left(\dfrac{n\pi x}{2b}\right) & x \le x' \\ e^{-n\pi x/2b}\cosh\left(\dfrac{n\pi x'}{2b}\right) & x \ge x' \end{cases} \tag{31}$$

We define function integrals of G_4 identical to the integrals (23) that applied to G_2. The reader may anticipate that this procedure leads to six functions identical to the previous functions Ξ_i, but expressed in terms of the odd-term series $\chi_{i\nu}$. To illustrate, the function Ξ_0 for Mode IV is

$$\Xi_0 = \int_\eta^\xi\int_\eta^\xi G_4(x, a \mid x', a)dx'dx$$
$$= \frac{2}{\epsilon b}\left[(\xi-\eta)\chi_{02} - \chi_{03} + \chi_{13} - \chi_{23} + \tfrac{1}{2}(\chi_{33} + \chi_{43})\right] \tag{32}$$

which may be compared to Ξ_0 for Mode II in (24).

The procedure to obtain Z_{04} is now obvious. Z_{04} *is given by (25) when* Ξ_i, a_1 and a_2 *are derived from the series* $\chi_{i\nu}$.

The computational procedure leading to the four modal solutions may be summarized as follows: For a given set of cell dimensions, twenty-five series $S_{i\nu}$ and twenty-five series $\chi_{i\nu}$ must be evaluated. The series $S_{i\nu}$ may be used to construct the functions Σ_i and Ξ_i. One obtains $\sqrt{\epsilon_r}\, Z_{01}$ from (20) using Σ_i and $\sqrt{\epsilon_r}\, Z_{02}$ from (25) using Ξ_i. In identical fashion, the series $\chi_{i\nu}$ may be used to construct the functions Σ_i and Ξ_i. In this case, $\sqrt{\epsilon_r}\, Z_{03}$ is obtained from (20) using Σ_i and $\sqrt{\epsilon_r}\, Z_{04}$ is obtained from (25) using Ξ_i. When calculations were carried out on an IBM 7094 computer, the computer was able to obtain 900 different solutions of mode impedance in less than two minutes of machine time.

Discussion of Results

Some interesting relations may be deduced from the variational formulation of the problem. In Fig. 4(a), we show a single strip conductor in a trough identical to the cell geometry of Fig. 3. The trough width is b, and the strip is located at a position $a=b/2$, midway between the parallel ground planes. In Fig. 4(b), we show a dual strip line in a trough of width b, where the conductors are energized in parallel (+, +) as shown. The strips are located at positions $a=b/4$ from the ground planes. The conductor widths $2w$ and displacements η from the end wall are assumed identical in Fig. 4(a) and (b). We shall now establish an exact relation between the impedances of the two configurations.

The Green's function for Fig. 4(a) is (3). The characteristic impedance is given by (20), where the functions Σ_i derive from the series $S_{i\nu}$. We consider the case $a=b/2$; thus, in the numerators of all of the series $S_{i\nu}$, the factor $\sin^2(ka)=\sin^2[n(\pi/2)]=1$ for $n=1, 3, 5 \ldots$ and $\sin^2(ka)$ vanishes for n even. Consequently, for this special case the series $S_{i\nu}$ reduce to odd-term series where the sine function in the numerator is equal to unity.

Now consider Fig. 4(b). The dashed line is a magnetic wall so that the lower "cell" is similar to the cell for Mode III defined in boundary conditions (26), except that the magnetic boundary is defined at $y=b$ in (26), and it is defined at $y=b/2$ in Fig. 4(b). The Green's function for a unit line source in the cell of Fig. 4(b) is

$$G(x, y \mid x', y') = \frac{4}{\epsilon\pi} \sum_{n=1,3,5,\cdots}^{\infty} \frac{1}{n} \sin\left(\frac{n\pi y}{b}\right) \sin\left(\frac{n\pi y'}{b}\right) \cdot \begin{cases} e^{-n\pi x'/b} \sinh\left(\dfrac{n\pi x}{b}\right) & x \le x' \\ e^{-n\pi x/b} \sinh\left(\dfrac{n\pi x'}{b}\right) & x \ge x' \end{cases} \quad (33)$$

which may be compared with (3), where (3) leads to the impedance of Fig. 4(a). Note that (33) is precisely two times (3), when (3) is restricted to the odd integers. We have already seen that (3), or more precisely $G_1(x, a \mid x', a)$ as defined in (6), becomes an odd-term series for the case $a=b/2$.

When one uses (33) to derive the cell impedance for Fig. 4(b), the solution is given by two times (20), where the functions Σ_i are constructed of series identical to the series $S_{i\nu}$ with the restriction that the series are summed only over the odd integers. For the geometry under consideration, $a=b/4$; thus, in all of the series numerators $\sin^2(ka)=\sin^2[n(\pi/4)]=1/2$, since $n=1, 3, 5, \cdots$ in (33).

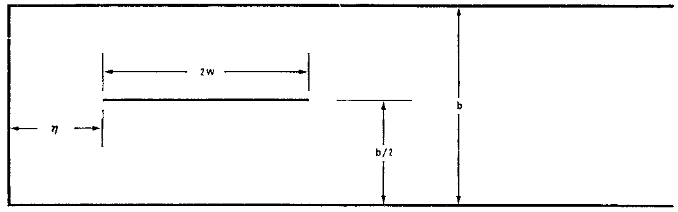

(a)

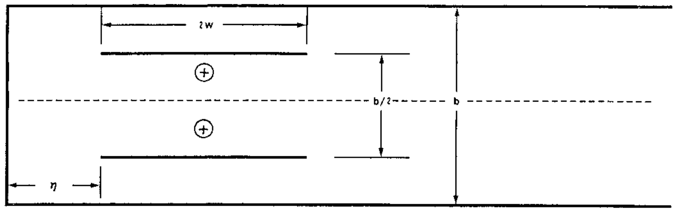

(b)

Fig. 4. (a) Single-strip trough transmission line. (b) Dual-strip trough transmission line.

It is now evident that, under the conditions specified, every series $S_{i\nu}$ that applies to the cell of Fig. 4(b) is precisely one-half times the identical series $S_{i\nu}$ that applies to Fig. 4(a). The series for the two configurations are identical except for a constant multiplier of one-half. The functions Σ_i are linear in the series $S_{i\nu}$ and so scale exactly by one-half. From (18) and (19), the variational parameters a_1 and a_2 are independent of a constant multiplier. It follows from (20) and the preceding discussion that the "cell impedance" of Fig. 4(b) is *identical* to the impedance of Fig. 4(a). The characteristic impedance of the entire dual strip line in Fig. 4(b), that is, the cell plus its image in the magnetic boundary, is one-half times the cell impedance. Thus, we establish that the dual strip-line impedance is exactly one-half times the single strip-line impedance. Correspondingly, the dual-strip capacitance per unit length is exactly twice the single-strip capacitance per unit length, and this characteristic is independent of the displacement η and the strip width $2w$. This rather remarkable property is made evident through the variational formulation of the problem. The result is exact because the variational solution is exact for an infinite series representation of the charge distribution, and all of the foregoing results still hold for an infinite series representation. As the strip displacement η becomes very large compared to the trough width, the impedances approach the values for an isolated strip[7] and broadside-coupled strips[8] between infinite parallel

[7] Collin, R. E., *op. cit.*, pp 139–143.

[8] Cohn, S. B., Characteristic impedances of broadside-coupled strip transmission lines, *IRE Trans. on Microwave Theory and Techniques*, vol MTT-8, Nov 1960, pp 633–637.

ground planes. Thus, the impedance relation may be verified for the limiting case $\eta/b \rightarrow \infty$ from these results. Because the Mode III solution was derived for a cell width of b in order for the geometry to be consistent with Fig. 1, it follows that Z_{03} for the dimensions $a/b=1/2$, $2\eta/b$, $2w/b$ will be identical to Z_{01} for the dimensions $a/b=1/2$, η/b, w/b.

The variational solution is an upper bound and, as such, is always somewhat greater than the exact characteristic impedance of the transmission line. In order to estimate the accuracy of the variational solutions, we let η/b becomes very large and compare Z_{01} and Z_{03} with Cohn's "odd" and "even" mode impedances for broadside-coupled strips. Cohn's solutions, which are obtained by an approximate conformal mapping of the problem, are valid for w/τ greater than about 0.35. In order to utilize the simplified (4) and (5),[9] the additional condition $(w/b)/(1-\tau/b) \geq 0.35$ must be satisfied. Selecting a range of line dimensions which satisfy these conditions ($w/b=0.5$, $0.1 \leq \tau/b \leq 0.9$), the variational solutions are compared with the conformal mapping solutions in Table I. Because of symmetry, Z_{01} at (τ/b) is equal to Z_{01} at $(1-\tau/b)$.

Specifying $a/b=1/2$, Z_{01} and Z_{02} are the odd and even mode impedances of two coplanar strips displaced midway between infinite parallel ground planes.[10] This problem may be solved exactly by means of conformal mapping. In Table II, we compare the variational solutions with the exact solutions for narrow ($w/b=0.05$) and wide ($w/b=0.5$) strips. The gap separation between the coplanar strips varies from 0.025 to infinity, that is, from an extremely small gap to the geometry of an isolated strip between parallel ground planes.

First we note that Z_{02} is within 2 per cent of the exact solution over the entire range of dimensions. The variational solution Z_{01} is accurate to within 2 per cent over a wide range of dimensions, but the error may exceed 2 per cent when the gap separation η/b becomes small. Evidently, the simple parabolic charge distribution is not an adequate representation for very closely spaced coplanar strips in a $(+, -)$ mode. Considering a constant width strip, the error increases as η/b decreases. Conversely, for a constant η/b, the error increases with the strip width w/b. The maximum error appearing in Table II is 11.6 per cent which results for $w/b=0.5$, $\eta/b=0.025$. Because Z_{03} is a $(+, -)$ coplanar mode similar to Z_{01}, the accuracy in determining Z_{03} should follow that of Z_{01}. Correspondingly, Z_{04} should be determined with the same order of accuracy as Z_{02}.

The variational solutions exceed the exact mode impedances by an amount that depends upon the mode and the relative line dimensions. By studying the data in Tables I and II, it is possible to estimate a "correction factor" to apply to the variational impedances so that they will nearly correspond to the exact values. Consider, for example, the odd and even mode impedances for broadside-coupled strips (Z_{01} and Z_{03} in Table I). If one divides the variational values by the factor 1.02, the variational and exact impedances are almost identical. The same factor holds for narrow-width strips. Referring to Table II, if the gap separation $\eta/b \geq 0.1$, the factor 1.02 adjusts Z_{01} to within 2 per cent of the exact impedance for both narrow and wide strip conductors. In fact, in most cases, the error is negligible. It is possible, of course, to obtain a lower bound variational solution in terms of an assumed potential distribution, and to thereby "bracket" the exact impedance of the line. The labor involved in this procedure is as great as for the upper bound solution and did not seem warranted in view of the accuracy of the upper bound solutions for most line dimensions.

Impedance data resulting from the variational analyses are presented in Figs. 5 through 16. In all cases, the quantity shown is $\sqrt{\epsilon_r}\, Z_0$ which is, of course, numerically identical to the characteristic impedance of an air dielectric ($\sqrt{\epsilon_r}=1$) transmission line excited in the given mode. Z_{01}, Z_{02}, Z_{03} and Z_{04} are "cell impedances" and, therefore, represent the characteristic impedance from one strip conductor to ground under the boundary conditions imposed by the particular mode of excitation illustrated in Fig. 2. In Figs. 5 through 9, we show $\sqrt{\epsilon_r}\, Z_{01}$ and $\sqrt{\epsilon_r}\, Z_{02}$ as functions of the normalized strip conductor width w/b. Each curve of impedance is for a constant gap separation η/b. The family of curves in each figure corresponds to a constant strip displacement τ/b between the broadside-coupled strips. The curve $\eta/b=\infty$ yields the impedance of a single isolated strip conductor between parallel planes, or of two broadside-coupled strip conductors between ground planes when excited in the odd mode. As mentioned above, the odd $(+, -)$ potential symmetry of Modes I and II about $y=b$ causes Z_{01} and Z_{02} at (τ/b) to be identical to Z_{01} and Z_{02}, respectively, at the symmetrical position $[1-(\tau/b)]$. Consequently, the five figures provide impedance data for (τ/b) over the interval $0.1 \leq (\tau/b) \leq 0.9$ in increments of 0.1.

In a similar fashion, curves of $\sqrt{\epsilon_r}\, Z_{03}$ and $\sqrt{\epsilon_r}\, Z_{04}$ are presented in Figs. 10 through 14 for $\tau/b=0.1$, 0.3, 0.5, 0.7, 0.9. The even $(+, +)$ potential symmetry of Modes III and IV about $y=b$ causes Z_{03}, Z_{04} at (τ/b) to be different from Z_{03}, Z_{04} at $[1-(\tau/b)]$. The curve $\eta/b=\infty$ yields the impedance of two broadside-coupled strip conductors between parallel planes when excited in the even mode.

The impedance data $\sqrt{\epsilon_r}\, Z_{01}$ and $\sqrt{\epsilon_r}\, Z_{03}$ for $\eta/b=\infty$ are collected in Figs. 15 and 16, respectively. These curves complement Cohn's solutions for broadside-coupled strips since they hold for dimensions beyond the range for which Cohn's formulas are valid.

[9] Cohn, S., *ibid.*, page 635.
[10] ——, Shielded coupled-strip transmission line, *IRE Trans. on Microwave Theory and Techniques*, vol MTT-3, Oct 1955, pp 29–38.

TABLE I

w/b	τ/b	Z_{01} Vari-ational,	Z_{01} Approxi-mate	Z_{03} Vari-ational,	Z_{03} Approxi-mate
0.5	0.1	28.7	28.1	173.0	169.6
↓	0.3	58.2	57.0	133.6	131.3
	0.5	66.7	65.4	102.2	100.2
	0.7	58.2	57.0	70.4	68.6
	0.9	28.7	28.1	30.0	29.1

TABLE II

w/b	η/b	Z_{01} Variational	Z_{01} Exact	Z_{02} Variational	Z_{02} Exact
0.05	0.025	102.8	98.4	285.6	282.5
↓	0.05	122.2	118.9	269.5	266.1
	0.10	146.5	143.4	247.3	245.6
	0.20	171.9	168.7	223.2	220.3
	0.45	193.4	189.3	203.7	199.7
	∞	199.0	195.0	199.0	195.0
0.50	0.025	51.1	45.8	76.9	75.7
↓	0.05	54.2	50.7	75.5	74.4
	0.10	58.3	56.0	73.3	72.2
	0.20	62.6	60.9	70.4	69.2
	0.45	66.0	64.5	67.5	66.2
	∞	66.7	65.4	66.7	65.4

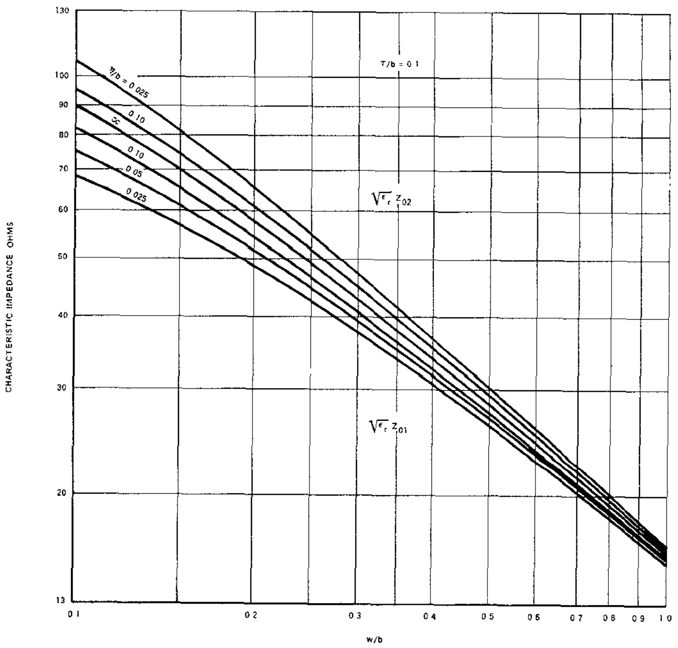

Fig. 5. $\sqrt{\epsilon_r}Z_{01}$ and $\sqrt{\epsilon_r}\,Z_{02}$ vs. w/b, η/b, for $\tau/b=0.1$.

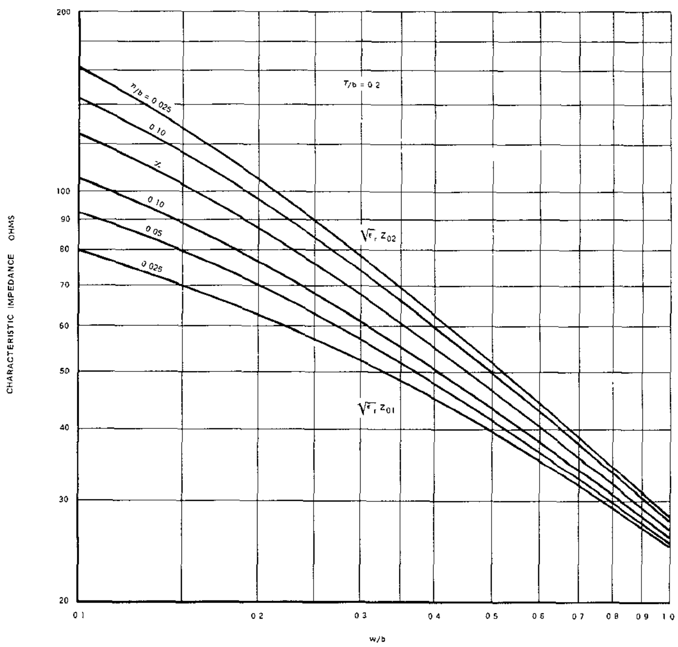

Fig. 6. $\sqrt{\epsilon_r}\,Z_{01}$ and $\sqrt{\epsilon_r}\,Z_{02}$ vs. w/b, η/b, for $\tau/b=0.2$.

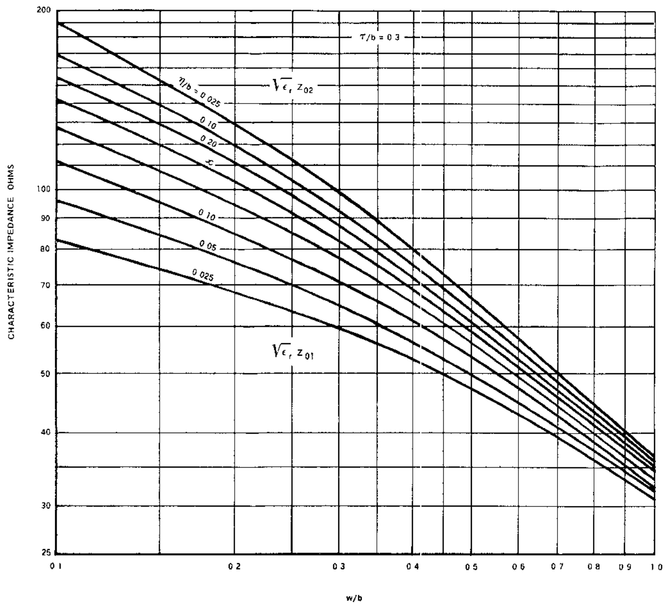

Fig. 7. $\sqrt{\epsilon_r}\, Z_{01}$ and $\sqrt{\epsilon_r}\, Z_{02}$ vs. w/b, η/b, for $\tau/b=0.3$.

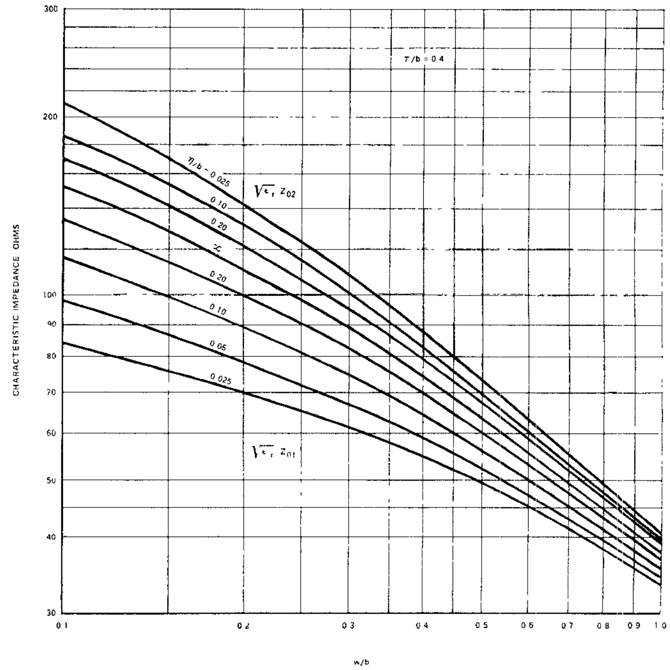

Fig. 8. $\sqrt{\epsilon_r}\, Z_{01}$ and $\sqrt{\epsilon_r}\, Z_{02}$ vs. w/b, η/b, for $\tau/b=0.4$.

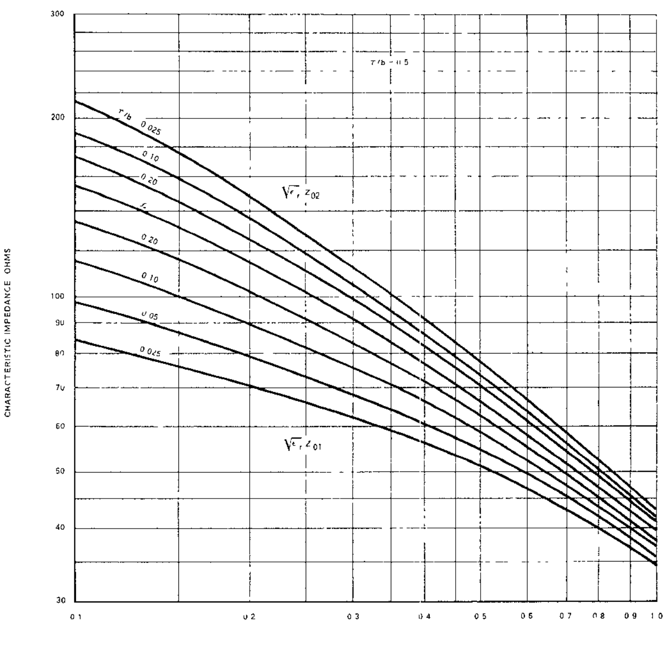

Fig. 9. $\sqrt{\epsilon_r}\, Z_{01}$ and $\sqrt{\epsilon_r}\, Z_{02}$ vs. w/b, η/b, for $\tau/b=0.5$.

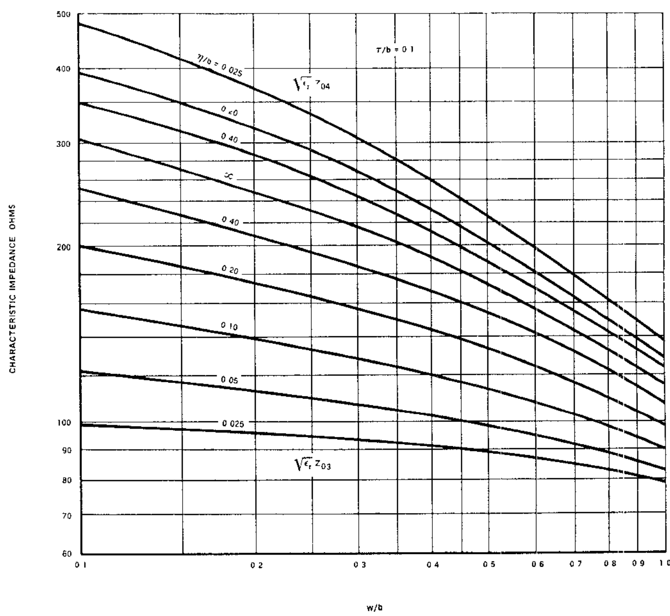

Fig. 10. $\sqrt{\epsilon_r}\, Z_{03}$ and $\sqrt{\epsilon_r}\, Z_{04}$ vs. w/b, η/b, for $\tau/b=0.1$.

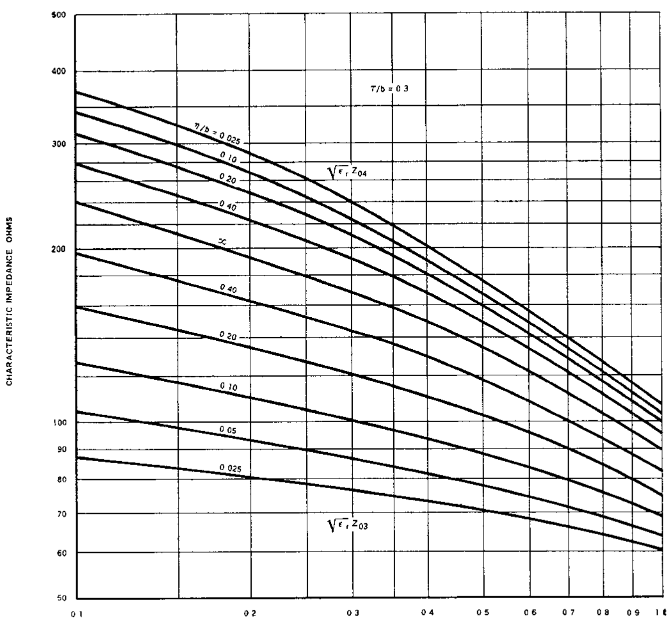

Fig. 11. $\sqrt{\epsilon_r}\,Z_{03}$ and $\sqrt{\epsilon_r}\,Z_{04}$ vs. w/b, η/b, for $\tau/b=0.3$.

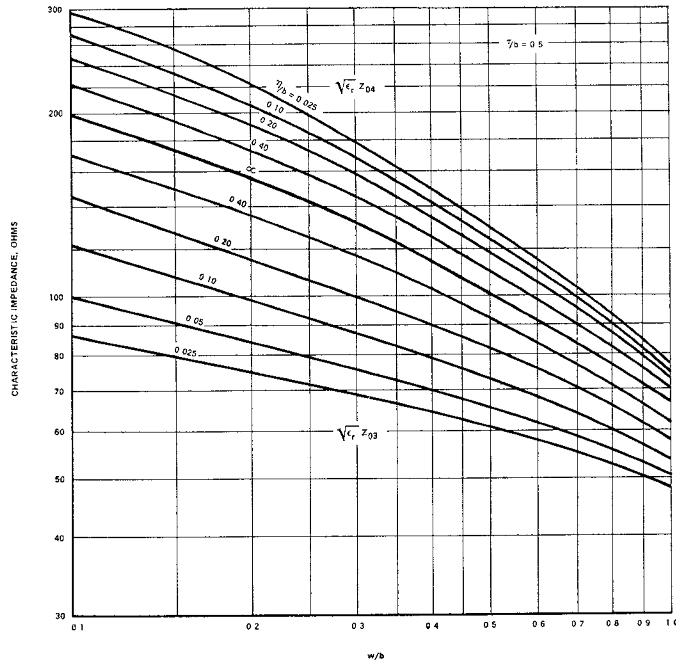

Fig. 12. $\sqrt{\epsilon_r}\,Z_{03}$ and $\sqrt{\epsilon_r}\,Z_{04}$ vs. w/b, η/b, for $\tau/b=0.5$.

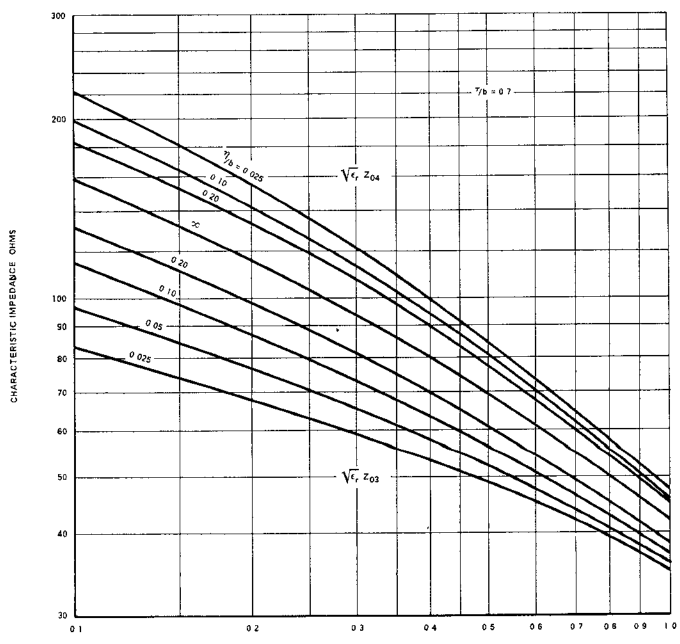

Fig. 13. $\sqrt{\epsilon_r}\,Z_{03}$ and $\sqrt{\epsilon_r}\,Z_{04}$ vs. w/b, η/b, for $\tau/b=0.7$.

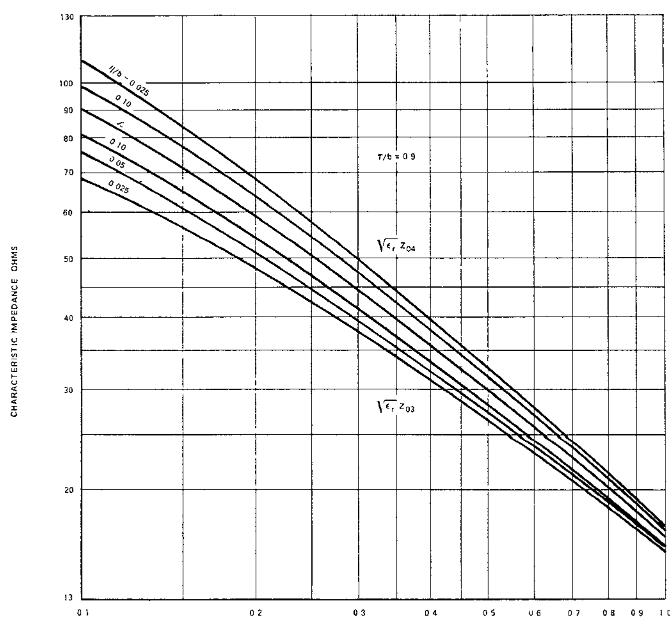

Fig. 14. $\sqrt{\epsilon_r}\,Z_{03}$ and $\sqrt{\epsilon_r}\,Z_{04}$ vs. w/b, η/b, for $\tau/b=0.9$.

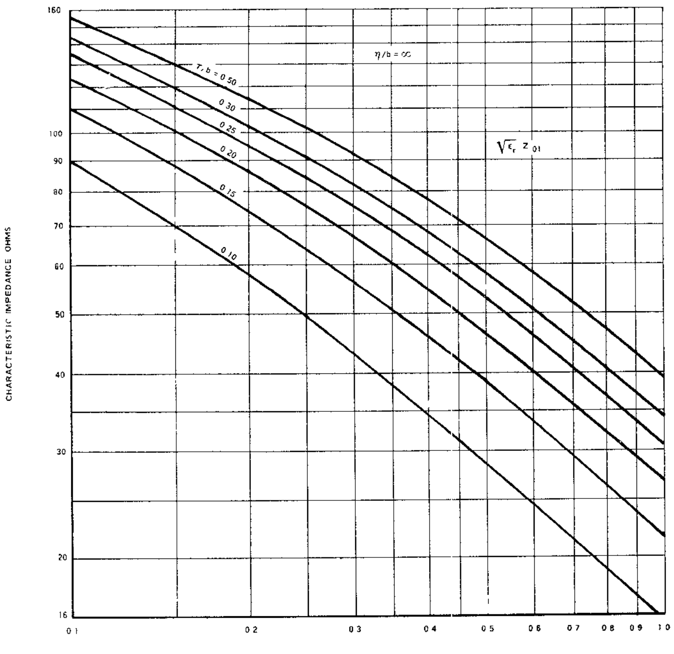

Fig. 15. $\sqrt{\epsilon_r}\, Z_{01}$ vs. w/b, τ/b, for $\eta/b=\infty$. (Odd Mode, two broadside-coupled strips.)

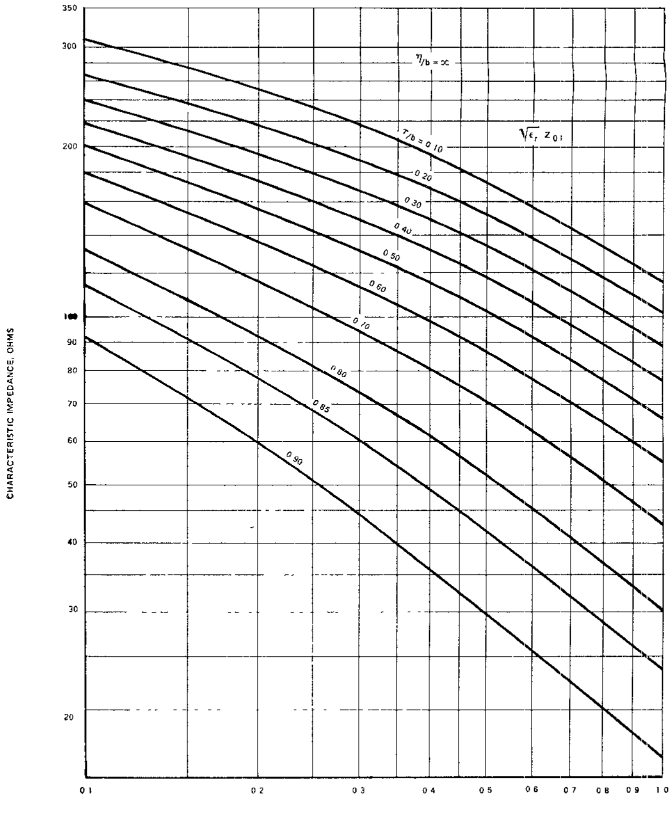

Fig. 16. $\sqrt{\epsilon_r}\, Z_{03}$ vs. w/b, τ/b, for $\eta/b=\infty$. (Even Mode, two broadside-coupled strips.)

Appendix

The integral definitions of the functions Σ_i and Ξ_i are given in (12) and (23). The functions are written below for corresponding indices as a single expression using the $(\pm)$ sign notation. Remember that Σ_i and Ξ_i also may be written using the series χ_{iv} as was shown in (28) and (32). This procedure leads to the solutions Z_{03} and Z_{04}. The functions Σ_i and Ξ_i are as follows:

$$\begin{matrix}\Sigma_0\\ \Xi_0\end{matrix} = \frac{2}{\epsilon b}\left[(\xi-\eta)S_{02} - S_{03} + S_{13} \pm S_{23} \mp \frac{1}{2}(S_{33}+S_{43})\right] \tag{34}$$

$$\begin{matrix}\Sigma_1\\ \Xi_1\end{matrix} = \frac{2}{\epsilon b}\left[\left(\frac{\xi^2-\eta^2}{2}\right)S_{02} - \frac{\xi}{2}(S_{03}-S_{13}\mp S_{23}\pm S_{33}) - \frac{\eta}{2}(S_{03}-S_{13}\mp S_{23}\pm S_{43}) \pm S_{24} \mp \frac{1}{2}(S_{34}+S_{44})\right] \tag{35}$$

$$\begin{matrix}\Sigma_2\\ \Xi_2\end{matrix} = \frac{2}{\epsilon b}\Bigg[\left(\frac{\xi^3-\eta^3}{3}\right)S_{02} - \frac{\xi^2}{2}(S_{03}-S_{13}\mp S_{23}\pm S_{33}) - \frac{\eta^2}{2}(S_{03}-S_{13}\mp S_{23}\pm S_{43}) + \xi(S_{04}+S_{14}\pm S_{24}\mp S_{34}) - \eta(S_{04}+S_{14}\mp S_{24}\pm S_{44}) - 2(S_{05}-S_{15}\mp S_{25}) \mp (S_{35}+S_{45})\Bigg] \tag{36}$$

$$\begin{matrix}\Sigma_3\\ \Xi_3\end{matrix} = \frac{2}{\epsilon b}\Bigg[\left(\frac{\xi^3-\eta^3}{3}\right)S_{02} - \frac{\xi^2}{2}(S_{03}\pm S_{33}) - \frac{\eta^2}{2}(S_{03}\pm S_{43}) + \xi\eta(S_{13}\pm S_{23}) - \xi(S_{14}\mp S_{24}\pm S_{34}) + \eta(S_{14}\pm S_{24}\mp S_{44}) + (S_{05}-S_{15}\pm S_{25}) \mp \frac{1}{2}(S_{35}+S_{45})\Bigg] \tag{37}$$

$$\left.\begin{aligned}\frac{\Sigma_4}{\Xi_4} = \frac{2}{\epsilon b}\Bigg[&\left(\frac{\xi^4-\eta^4}{4}\right)S_{02} + \left(\frac{\xi^2\eta+\xi\eta^2}{2}\right)(S_{13}\pm S_{23}) - \frac{\xi^3}{2}(S_{03}\pm S_{33}) - \frac{\eta^3}{2}(S_{03}\pm S_{43}) \pm 2\xi\eta S_{24}\\ &+\frac{\xi^2}{2}(S_{04}-S_{14}\pm S_{24}\mp 3S_{34}) - \frac{\eta^2}{2}(S_{04}-S_{14}\mp S_{24}\pm 3S_{44}) \pm 2\xi(S_{25}-S_{35})\\ &\pm 2\eta(S_{25}-S_{45}) \pm (2S_{26}-S_{36}-S_{46})\Bigg]\end{aligned}\right\} \quad (38)$$

$$\left.\begin{aligned}\frac{\Sigma_5}{\Xi_5} = \frac{2}{\epsilon b}\Bigg[&\left(\frac{\xi^5-\eta^5}{5}\right)S_{02} + \xi^2\eta^2(S_{13}\pm S_{23}) - \frac{\xi^4}{2}(S_{03}\pm S_{33}) - \frac{\eta^4}{2}(S_{03}\pm S_{43}) - 2\xi^2\eta(S_{14}\mp S_{24}) + 2\xi\eta^2(S_{14}\pm S_{24})\\ &+\frac{2\xi^3}{3}(S_{04}\mp 3S_{34}) - \frac{2\eta^3}{3}(S_{04}\pm 3S_{44}) - 4\xi\eta(S_{15}\mp S_{25}) + 2\xi^2(S_{15}\pm S_{25}\mp 2S_{35}) + 2\eta^2(S_{15}\pm S_{25}\mp 2S_{45})\\ &+4\xi(S_{16}\pm S_{26}\mp S_{36}) - 4\eta(S_{16}\mp S_{26}\pm S_{46}) - 2(2S_{07}-2S_{17}\mp 2S_{27}\pm S_{37}\pm S_{47})\Bigg]\end{aligned}\right\} \quad (39)$$

The series $S_{i\nu}$ and $\chi_{i\nu}$ are, in general, functions of the variables a, b, $\xi=(h+w)$, and $\eta=(h-w)$. The argument of the sine function in the $S_{i\nu}$ series is $(ka)=n\pi a/b$. The argument of the sine function in the $\chi_{i\nu}$ series is $(ka/2)$. The subscript i denotes a family of series, all of which contain the same exponential factor. For example, $e^{-k(\xi+\eta)}$ occurs in all of the series $S_{2\nu}$. The subscript $i=0$ is used when no exponential factor is present. The subscript ν is the exponent or power of k that appears in the denominator of the general series term. The subscript ν takes on five different values for a particular i, and the subscript i takes on five values so that the double subscript notation identifies twenty-five series $S_{i\nu}$ and twenty-five series $\chi_{i\nu}$. In all of the series, $k=n\pi/b$ and $0<a<b$.

The five series $S_{0\nu}$ and the five series $\chi_{0\nu}$ are defined as follows:

$$S_{0\nu} = \sum_{n=1}^{\infty} \frac{\sin^2(ka)}{k^\nu} \quad (40)$$

$$\chi_{0\nu} = \sum_{n=1,3,5,\cdots}^{\infty} \frac{\sin^2(ka/2)}{(k/2)^\nu} = 2^\nu \sum_{n=1,3,5,\cdots}^{\infty} \frac{\sin^2(ka/2)}{k^\nu} \quad (41)$$

where $\nu=2, 3, 4, 5, 7$. We point out a characteristic that is evident in (40) and (41) which holds for all of the series under discussion. Any series $\chi_{i\nu}$ may be written from the corresponding series $S_{i\nu}$ by replacing k by $k/2$ everywhere, and restricting the summation to the odd integers. The exponent ν does not take on the value 2 in the remaining series, but does assume the value 6 which was not true with the series $S_{0\nu}$. In the following series, $\nu=3, 4, 5, 6, 7$. We define

$$S_{1\nu} = \sum_{n=1}^{\infty} \frac{\sin^2(ka)e^{-k(\xi-\eta)}}{k^\nu} \quad (42)$$

$$\chi_{1\nu} = 2^\nu \sum_{n=1,3,5,\cdots}^{\infty} \frac{\sin^2(ka/2)e^{-k(\xi-\eta)/2}}{k^\nu} \quad (43)$$

$$S_{2\nu} = \sum_{n=1}^{\infty} \frac{\sin^2(ka)e^{-k(\xi+\eta)}}{k^\nu} \quad (44)$$

$$\chi_{2\nu} = 2^\nu \sum_{n=1,3,5,\cdots}^{\infty} \frac{\sin^2(ka/2)e^{-k(\xi+\eta)/2}}{k^\nu} \quad (45)$$

$$S_{3\nu} = \sum_{n=1}^{\infty} \frac{\sin^2(ka)e^{-2k\xi}}{k^\nu} \quad (46)$$

$$\chi_{3\nu} = 2^\nu \sum_{n=1,3,5,\cdots}^{\infty} \frac{\sin^2(ka/2)e^{-k\xi}}{k^\nu} \quad (47)$$

$$S_{4\nu} = \sum_{n=1}^{\infty} \frac{\sin^2(ka)e^{-2k\eta}}{k^\nu} \quad (48)$$

$$\chi_{4\nu} = 2^\nu \sum_{n=1,3,5,\cdots}^{\infty} \frac{\sin^2(ka/2)e^{-k\eta}}{k^\nu} \quad (49)$$

The series S_{02}, χ_{02}, S_{04}, χ_{04} have closed-form expressions. The series S_{03}, χ_{03}, S_{05}, χ_{05} have alternate, more rapidly converging forms. The reader is directed to the formal report by Duncan[3] for details.

Acknowledgment

The author is pleased to acknowledge the constructive comments of R. H. DuHamel whose original studies of log-periodic circuit elements established the need for the strip-line analysis. N. Joy of Hughes Aircraft Co., Systems and Mathematical Analysis Section programmed the problem for solution on the digital computer. The manuscript was typed by Mrs. L. Schenet.